# Spectra of Raman scattering by waveguide and interference modes of a free GaP film

V. N. Denisov, T. A. Leskova, B. N. Mavrin, and V. B. Podobedov

*Spectroscopy Institute, USSR Academy of Sciences*
(Submitted 22 September 1987)
Zh. Eksp. Teor. Fiz. **94**, 261–273 (May 1988)

Polarized spectra of Raman scattering (RS) by waveguide and interference (virtual) modes of GaP films $6.8 \pm 0.5$ and $10.5 \pm 0.5\,\mu$m thick were obtained in the 300–500 $cm^{-1}$ range at scattering angles 0.5–4.5° and with angular resolution 0.25°. Four lower branches of waveguide $p$-type modes ($m = 1, 2, 3, 4$) and three $s$-type modes ($m = 1, 2, 3$) were obtained below the $TO$-phonon frequency, as well as two upper branches ($m = 1, 2$) of each type below the $LO$ phonon. It is shown that the intensity of $p$-modes with polarization $E_\perp$ is substantially lower than with polarization $E_\parallel$. A lower branch was observed of $m = 3$ interference modes whose bandwidths, owing to radiative damping, are twice as large as those of the waveguide modes. Roughness of the surface is shown to make no substantial contribution to the widths of the waveguide modes. Expressions are obtained for the RS spectrum of a crystal film, and the calculated spectra of a GaP film are given and compared with experiment.

## 1. INTRODUCTION

The presence of crystal boundaries alters substantially the vibrational spectrum in the bulk of a crystal.[1–4] In thin crystalline films are produced various classes of vibrational polaritons that are in either nonradiative or radiative states. Nonradiative excitations correspond to waves localized near the interface of two media (surface polaritons) and trapped inside the film (waveguide modes (WM)). Radiative vibrations are accomplished by emission of electromagnetic energy and correspond to virtual or interference modes (IM). Surface polaritons have been actively investigated by various methods, including Raman scattering (RS) (see Ref. 4, Chap. 12, and Ref. 5).

If surface polaritons are bound to the boundary and are consequently missing from the bulk-vibration spectrum, the appearance of WM and IM is indeed a reflection of the result of the action of the boundaries on the spectrum of the bulk polaritons, causing the single branch of transverse bulk polaritons to be replaced by two families ($p$-polarized (or TM) and $s$-polarized (or $TE$) modes) of an infinite number of WM and IM branches. The uncertainty of the normal component of the wave vector from WM and IM, which can amount to $\sim m\pi/d$ ($d$ is the film thickness, $m = 0, 1, 2, \ldots$), leads not only to the onset of families of WM and IM, but also to activity of dispersion-curve sections which are forbidden for Raman scattering in the case of strict satisfaction of the momentum-conservation law. For example, bulk polaritons on the upper branch of a cubic crystal are always forbidden in RS. An interesting observation was made in an investigation of IM and IR absorption.[7] It was shown that at resonance between IM and impurity-atom vibrations it is possible to increase the density sensitivity substantially. We note in this connection that since the WM and IM frequencies cover a broad spectral range and can be easily verified by changing the film thickness, the WM and IM can play a major role in vibrational spectroscopy of crystalline films.

WM and IM have already been investigated earlier theoretically and experimentally. The WM and IM dispersion laws were established in the pioneering theoretical studies,[1] where the radiative damping of the IM and IR absorption was investigated. The cross section for RS by WM and IM was also investigated earlier.[8] However, as noted in a later paper,[6] where results of a numerical analysis of the RS spectra were presented, the original paper contained errors. To compare experiment with theory it is therefore necessary to repeat the theoretical analysis of the RS cross section, with the errors eliminated.

Although RS and WM have already been investigated earlier for both free films[9] and films covered with diffraction gratings, many features could not be experimentally observed in RS, since the spectra were obtained without separating the $p$ and $s$ modes with very low resolution of the individual modes. Nor were polarization spectra investigated, so that it was impossible to obtain individually the $p$- and $s$-mode spectra. No IM were observed at all, nor were WM and IM observed in the dispersion region where the momentum is not conserved. There were no investigations of WM and IM damping. It is also of interest to compare the observed spectra of RS by WM and IM with those calculated for the experimental scattering geometries. In Sec. 2 below we consider the conditions for the observation of RS by WM and IM, derive expressions for the RS cross section and for the damping by vibrational polaritons of a thin film, and present the calculation results for a free GaP film. The experimental conditions are described in Sec. 3. The experimental RS spectra of the GaP film are discussed and compared with the calculation results in Sec. 4.

## 2. WAVEGUIDE AND INTERFERENCE MODES IN CRYSTALLINE FILMS

### 2.1 Some properties of waveguide and interference modes

We assume hereafter that the cubic-crystal film of thickness $d$ is located in a vacuum, and that in accordance with the experiment (see Sec. 3) the exciting radiation is normally incident on the film surface.

A feature of waveguide modes is that they form standing waves inside the film and are exponentially attenuated on the outside.[1] In other words, the WM undergo total internal reflection (TIR) from the crystal-vacuum interface. It is therefore possible to investigate WM in RS if the RS is ob-

 0038-5646/88/051013-08$04.00  

served at scattering angles $\theta' > \theta'_{cr}$ inside the crystal, where $\theta'_{cr}$ is the scattering angle when the angle between the wave vector $\mathbf{k}$ of the excited vibration and the crystal-vacuum interface is equal to the TIR angle $\varphi_0$. Since $\sin^2\varphi_0 = 1/n^2$ ($n$ is the refractive index of the crystal at the frequency $\omega$) and $\sin\varphi = k_\parallel/k$ (Fig. 1), the component $k_\parallel^0$ parallel to the surface, at which TIR takes place, is equal to $k/n$. Since $k = \omega n/c$, we have

$$k_\parallel^0 = \omega/c. \tag{1}$$

If $k_\parallel > k_\parallel^0$, total internal reflection takes place, so that excitations with these values of $k_\parallel$ are WM. The IM are excited if $k_\parallel < k_\parallel^0$. The plot of (1) is the light line and divides the $\omega k_\parallel$ plane into two parts, with the nonradiative modes on the right and the radiative ones on the left. Since the angles measured in experiment are the scattering angles $\theta$ outside the crystal, it is convenient to use the angle $\theta_{cr}$ defined by

$$\sin\theta_{cr} = \omega/\omega_s.$$

Here and below the subscript $s$ refers to the scattered radiation and $L$ to the exciting one. WM should be observed in the RS spectra at $\theta > \theta_{cr}$ and IM at $\theta \leqslant \theta_{cr}$. If $\omega = 350\ \mathrm{cm}^{-1}$ we have $\theta_{cr} \simeq 1$.

The dispersion curves $\omega(k_\parallel)$ for WM and IM are defined by the equations[1]

$$f = \frac{k_\perp}{\varkappa}\mathrm{tg}\left(\frac{k_\perp d}{2}\right), \quad f = -\frac{k_\perp}{\varkappa}\mathrm{ctg}\left(\frac{k_\perp d}{2}\right), \tag{2}$$

where $f = \varepsilon(\omega)$ for the $p$ modes and $f = 1$ for the $s$ modes,

$$\varkappa = (k_\parallel^2 - \omega^2/c^2)^{1/2}, \quad k_\perp = (\varepsilon\omega^2/c^2 - k_\parallel^2)^{1/2}, \quad k_\parallel = (\omega_L - \omega)\sin\theta/c.$$

In the case of IM we have $k_\parallel < \omega/c$ and furthermore $\omega$ becomes complex, making the solution of (2) more complicated. The solutions of the first equation of (2) are the even modes ($m = 0, 2, 4, \ldots$) and of the second the odd ones ($m = 1, 3, \ldots$). The following conclusions can be drawn from an analysis of Eqs. (2).

Although $k_\perp$ is a continuous function of the frequency, Eqs. (2) have an infinite number of solutions but only for certain discrete values of $k_\perp$ spaced a distance $\sim\pi/d$ apart.[3] Accordingly we have two families ($p$ and $s$ modes) with infinite WM and IM dispersion branches. In turn, each of the WM and IM types ($p$ and $s$) breaks up into two sets of branches: the lower branches, below the transverse-phonon frequency $\omega_{TO}$, and the upper above the longitudinal-phonon frequency $\omega_{LO}$. The lower and upper branches are bounded from below by the curve $k_\perp = 0$, i.e.,

$$k_\parallel = \omega\varepsilon^{1/2}/c. \tag{3}$$

The lower branches are thus located between the lower curve (3) and $\omega_{TO}$, but there is no upper bound for the upper branches. Given the scattering angle $\theta$ and hence $k_\parallel$, the $s$-mode frequencies are always lower than those of the $p$ modes both on the lower and on the upper branches.

The frequency interval $\Delta\omega$ between neighboring curves on the lower and upper branches depends on the film thickness and on its dielectric constant ($\Delta\omega \sim d^{-1}\varepsilon^{-1/2}$). According to Refs. 1 and 3, the lower branches condense with increase of the branch number $m$, and for the upper branches $\Delta\omega$ increases with increase of $m$.

## 2.2 SCATTERING CROSS SECTION AND RS LINEWIDTH IN THE WAVEGUIDE AND INTERFERENCE MODES

We have calculated the RS cross section using the fluctuation-dissipation theorem.[11] In the presence of a fluctuating field, the nonlinear polarization at the frequency $\omega_s$ of radiation scattered in polar crystals such as GaP is given by

$$P_i(\omega_s) = (a_{ijk}u_k^* + b_{ijk}E_k^{*p})E_j^L, \tag{4}$$

where $a_{ijk}$ is the tensor of the strain contribution to the RS, $b_{ijk}$ the electrooptic tensor, $u$ the relative displacement of the ions, and $E^p$ the electric field of the vibrational polariton. Using $P(\omega_s)$ in the form (4) we have solved in the given-field approximation the Maxwell equations with account taken of the boundary conditions, and determined the amplitudes of the field of frequency $\omega_s$ outside the crystal. The squares of the obtained amplitudes were then averaged over the possible values of $u(\mathbf{r},t)$ and $E_p(\mathbf{r},t)$. The amplitudes $u$ and the field $E^p$ were determined by simultaneously solving the equations of motion and the Maxwell equations in the presence of fluctuation forces. Averaging yielded the following expression for the doubly differential RS:

$$\frac{\partial^2\sigma}{\partial\Omega\,\partial\omega_s} = \frac{\hbar\omega_s^3\omega_L S}{\pi^2c^3\cos\theta}[n(\omega)+1]\,|t_L t_s|^2\,\mathrm{Im}(J_1+J_2), \tag{5}$$

where $t_L$ and $t_s$ are the amplitude transmission coefficients of the film, $\theta$ the scattering angle, and $S$ the area of the illuminated part of the sample. In the derivation of (5), the tensors $a_{ijk}$ and $b_{ijk}$ were represented in the form

$$(a, b)_{ijk} = (a, b)e_i^s e_j^L e_k^p,$$

where the vectors $\mathbf{e}^s$, $\mathbf{e}^L$ and $\mathbf{e}^p$ were determined by the scattering geometry. The term $J_1$ in (5) is given by

$$J_1 = \frac{\chi^2\omega^2/c^2}{2k_\perp D(k_\parallel,\omega)\sin(k_\perp d)}\left\{\left(f^2 + \frac{k_\perp^2}{\varkappa^2}\right)\chi(k_\perp)\chi(-k_\perp)\right.$$
$$\times[\gamma(k_\perp)\gamma^*(-k_\perp)\exp(ik_\perp d) + \gamma^*(k_\perp)\gamma(-k_\perp)\exp(-ik_\perp d)]$$
$$-\left(f - i\frac{k_\perp}{\varkappa}\right)^2\exp(-ik_\perp d)\,[\chi^2(k_\perp)\gamma(k_\perp)\gamma^*(k_\perp)$$
$$\left.+\chi^2(-k_\perp)\gamma(-k_\perp)\gamma^*(-k_\perp)]\right\} \tag{6}$$

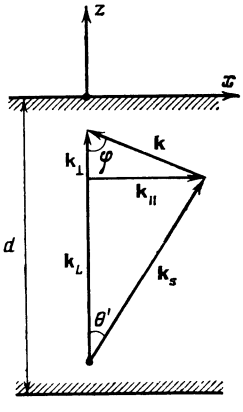


FIG. 1. Schematic representation of the RS process in a film of thickness $d$. The symbols are defined in the text.

Here $\chi = a(\varepsilon - \varepsilon_\infty) + b$; for $p$-polarized modes

$$\chi(q) = e_y^p q/(q^2+k_\parallel^2)^{1/2} - e_z^p k_\parallel/(q^2+k_\parallel^2)^{1/2},$$

and for $s$-polarized modes $\chi(q) = e_x^p$. The function $\gamma(q)$ is of the form

$$\gamma(q) = \frac{1-\exp[i(v-q)d]}{v-q} - r_s \frac{1-\exp[i(w-q)d]}{w-q}$$

$$-r_L \frac{1-\exp[-i(w+q)d]}{w+q} + r_L r_s \frac{1-\exp[-i(v+q)d]}{v+q}$$

$$\equiv \gamma_0(q) - \exp(-iqd)\gamma_1(q).$$

where $v = k_L - k_s$, $w = k_L + k_s$, $k_L$ ($k_s$), and $r_L$ ($r_s$) are the $z$ components of the wave vectors and the reflection coefficients of the exciting (scattered) radiation.

The term $J_z$ in (5) is of the form

$$J_2 = \frac{\varepsilon''|\chi_\perp(v)|^2}{(v^2-k_\perp^2)(v^2-k_\perp^{*2})}[\chi^2(v)\gamma^*(v) - \chi^2(-v)\gamma^*(-v)r_L r_s]$$
$$+ \frac{\varepsilon''|\chi_\perp(w)|^2}{(w^2-k_\perp^2)(w^2-k_\perp^{*2})}[\chi^2(-w)\gamma^*(-w)r_L - r_s\chi^2(w)\gamma^*(w)]$$
$$-i\frac{\chi^2\omega^2/c^2}{4k_\perp}\{\chi^2(-k_\perp)[\gamma_0(-k_\perp)\gamma^*(-k_\perp) - \gamma_1^*(-k_\perp)\gamma(-k_\perp)$$
$$\times\exp(-ik_\perp d)] + \chi^2(k_\perp)[\gamma_0^*(k_\perp)\gamma(k_\perp) - \gamma_1(k_\perp)\gamma^*(k_\perp)$$
$$\times\exp(-ik_\perp d)]\} + \frac{\varepsilon''}{|\varepsilon|^2}[\chi_{LO}^2(v)\gamma^*(v) - r_L r_s\chi_{LO}^2(-v)\gamma^*(-v)$$
$$+ r_L\chi_{LO}^2(-w)\gamma^*(-w) - r_s\chi_{LO}^2(w)\gamma^*(w)], \tag{7}$$

where

$$\chi_\perp(q) = a[(q^2+k_\parallel^2)c^2/\omega^2 - \varepsilon_\infty] + b,$$

and for $p$-polarized modes

$$\chi_{LO}(q) = (-a\varepsilon_\infty + b)[e_y^p k_\parallel/(q^2+k_\parallel^2)^{1/2} + e_z^p q/(q^2+k_\parallel^2)^{1/2}],$$

whereas $\chi_{LO}(q) = 0$ for $s$-polarized modes. Note that the cross section for backward RS is determined by expression (5) with $J_1$ and $J_2$ given by Eqs. (6) and (7), in which $k_s$ must be replaced by $-k_s$.

The term $J_1$ has maxima at the frequencies of the eigenmodes of the film (at the frequencies of the surface polaritons, WM and IM). This is due to the presence, in the denominator of (6), of the function

$$D(k_\parallel, \omega) = \left(f - \frac{k_\perp}{\varkappa}\operatorname{tg}\frac{k_\perp d}{2}\right)\left(f + \frac{k_\perp}{\varkappa}\operatorname{ctg}\frac{k_\perp d}{2}\right), \tag{8}$$

which vanishes in the absence of damping at the frequencies of the eigenmodes of the film. The term $J_2$ describes scattering by film bulk excitations ($TO$, $LO$) perturbed by the presence of the boundaries. Both terms contain the functions $\gamma(q)$ that attest to the violation of the momentum conservation in the bounded system.

In the weak-damping limit, the cross section by RS by the eigenmodes of the film can be written in the form

$$\frac{\partial^2\sigma}{\partial\Omega\,\partial\omega_s} = \frac{\hbar\omega_s^3\omega_L S}{2\pi^2 c^3\cos\theta}[n(\omega)+1]|t_L t_s|^2 \frac{\chi^2|\varkappa|\omega^2/c^2}{k_\perp^2|\Psi(k_\parallel)|}$$
$$\times\left|\left(f + i\frac{k_\perp}{\varkappa}\right)\chi(-k_\perp)\gamma(-k_\perp) - \left(f - i\frac{k_\perp}{\varkappa}\right)\gamma(k_\perp)\chi(k_\perp)\right|^2 \frac{\gamma/2}{(\omega-\omega_n)^2+\gamma^2/4}, \tag{9}$$

where $\omega_n$ is the solution of the equation $D(k_\parallel, \omega) = 0$ with damping disregarded, and

$$\Psi(k_\parallel) = \frac{\omega}{c^2}\left[\frac{\varepsilon f}{k_\perp^2} + \frac{f}{\varkappa^2} + \frac{d}{2\varkappa}\varepsilon\left(1 + f^2\frac{\varkappa^2}{k_\perp^2}\right)\right]$$
$$+ \frac{d\varepsilon}{d\omega}\left\{\frac{1}{2}\frac{\omega^2}{c^2}\left[\frac{f}{k_\perp^2} + \frac{d}{2\varkappa}\left(1 + f^2\frac{\varkappa^2}{k_\perp^2}\right)\right] - f_0\right\}\Big|_{\omega=\omega_n}.$$

The half-width $\gamma$ of the line of RS by surface polaritons is determined in the WM by the expression

$$\gamma = \Gamma/(1+G), \tag{10}$$

where $\Gamma$ is the phonon damping and

$$G = \frac{\omega}{c^2}\left[\frac{\varepsilon f}{k_\perp^2} + \frac{f}{\varkappa^2} + \frac{d}{2\varkappa}\varepsilon\left(1 + f^2\frac{\varkappa^2}{k_\perp^2}\right)\right]\left\{\frac{d\varepsilon}{d\omega}\left[\frac{1}{2}\frac{\omega^2}{c^2}\left(\frac{f}{k_\perp^2} + \frac{d}{2\varkappa}\left(1 + f^2\frac{\varkappa^2}{k_\perp^2}\right)\right) - f_0\right]\right\}^{-1}\Big|_{\omega=\omega_n}. \tag{11}$$

Here and below, $f_0 = 1$ for $p$-polarized modes and $f_0 = 0$ for $s$-polarized modes.

In the case of RS by WM we have $\varkappa = -ik$ and in the free-damping limit the RS cross section takes the form (9) in which, however, the function $\Psi(k_\parallel)$ is given by

$$\Psi(k_\parallel) = f\frac{\omega}{c^2}\left(\frac{\varepsilon}{k_\perp^2} - \frac{1}{k^2}\right) + \frac{d\varepsilon}{d\omega}\left(\frac{1}{2}\frac{\omega^2}{c^2}\frac{f}{k_\perp^2} - f_0\right)\Big|_{\omega=\omega_n'}.$$

In this case the frequency $\omega_n$ is complex: $\omega_n = \omega_n' - i\omega_n''$, $\omega_n'' > 0$, $\omega_n''$ is the radiation damping. The line half-width for RS and IM is given by

$$\gamma = 2\omega_n'' + \Gamma/(1+G_1), \tag{12}$$

where

$$G_1 = f\frac{\omega}{c^2}\left(\frac{\varepsilon}{k_\perp^2} - \frac{1}{k^2}\right)\left[\frac{d\varepsilon}{d\omega}\left(\frac{1}{2}\frac{\omega^2}{c^2}\frac{f}{k_\perp^2} - f_0\right)\right]^{-1}\Big|_{\omega=\omega_n'}.$$

We have calculated the spectra of the RS by the natural oscillations of a GaP film oriented in accordance with Sec. 3, for scattering geometries in one of which $p$-polarized modes are active (geometry 7 in the table), and in the other $s$-polarized modes (geometry 8 in the table). We used in the calculations the experimental many-oscillator function of the GaP dielectric constant,[12] as well as the refractive index of the GaP in the visible region (5300–5500 Å) in the form

$$n = 3.4522 + 8180(1/\lambda_s - 1/5450),$$

TABLE I. Types of waveguide and interference modes active in the RS spectra at different scattering geometries.

| No. | Exciting-field direction | Wave-vector direction | Scattering-tensor component | Type of mode* |
|---|---|---|---|---|
| 1 | $\mathbf{E}_L \parallel \mathbf{x}$ | $\mathbf{k}_\parallel \parallel \mathbf{x}$ | $I_{xx}$ | $s^y+p^z$ |
| 2 | | | $I_{xy}$ | $p^x$ |
| 3 | | $\mathbf{k}_\parallel \parallel \mathbf{y}$ | $I_{xx}$ | $p^y+p^z$ |
| 4 | | | $I_{xy}$ | $s^x$ |
| 5 | $\mathbf{E}_L \parallel \mathbf{y}$ | $\mathbf{k}_\parallel \parallel \mathbf{x}$ | $I_{yy}$ | $s^y+p^z$ |
| 6 | | | $I_{yx}$ | $p^x$ |
| 7 | | $\mathbf{k}_\parallel \parallel \mathbf{y}$ | $I_{yy}$ | $p^y+p^z$ |
| 8 | | | $I_{yx}$ | $s^x$ |

*The superscripts of the $p$ and $s$ modes indicate the directions of the polarization vector $E^p$.

where $\lambda_s$ is the wavelength in Å. This $n(\lambda_s)$ dependence was determined by us from investigations of the bulk-polariton spectrum. Although the calculated spectra contain also surface polaritons (between $\omega_{TO}$ and $\omega_{LO}$), we shall discuss below only WM and IM.

The qualitative changes of the spectrum of the GaP bulk polaritons with decrease of the film thickness are similar to those observed in Refs. 5 and 6 and discussed in Sec. 2.1. For thick films ($d \gtrsim 100\ \mu$m) the distance between the WM and IM branches is small, the uncertainty ($\Delta k \sim \pi/d$) of the WM and IM wave vectors is as yet also small, therefore the spectrum shows only one line at the frequency of the bulk polariton. With decrease of the thickness, the values of $\Delta k$ and $\Delta\omega$ increase, and at $d \lesssim 30\ \mu$m one can see in the spectrum several WM and IM modes of comparable intensity in place of the single bulk-polariton line. The relative intensities of the modes are determined not only by the geometric factor that depends on $\Delta k$, but also substantially by the frequency dependence of the susceptibility $\chi(\omega)$, which usually varies greatly near the lattice resonances $\omega_{TO}$ and $\omega_{LO}$ (Ref. 13).

The calculated RS spectra for the eigenmodes of a film $6.8 \pm 0.5\ \mu$m thick are shown in Fig. 2. The most interesting feature of these spectra is that not more than three or four branches are observed in the region of the lower branches. Branches with $m > 4$ are manifested as a shoulder of the *TO* phonon, visible on account of reflection from the rear surface of the film. The reason is that at $m > 3$ the distance between the branches becomes smaller than the widths of the WM and IM lines. There is no mode with $m = 0$ in the calculated spectra. The bands on the lower branches become narrower with decrease of $m$, owing to the corresponding decrease of the imaginary part $\varepsilon''(\omega)$. At $\theta < \theta_{cr}$, however, when the IM rather than the WM become intense, the bands broaden and attest to the contribution of the radiative damping to the widths of the bands. The dispersion of the WM on the upper branch is large, so that a strong shift of the WM frequency is expected when $\theta$ is changed.

### 3. DESCRIPTION IS EXPERIMENT

The spectra of the RS by WM and IM were excited and recorded by using the second harmonic of a pulsed YAG:$Nd^{3+}$ laser with high repetition frequency, a triple polychromator (a double premonochromator and DFS-4 spectrograph), and a multichannel recording system.[5] Depending on the grating employed, the DFS-4 recorded simultaneously a 150- or 300-$cm^{-1}$ section with resolution $\approx 3$ or $\approx 6\ cm^{-1}$. To investigate the WM and IM damping, the DFS-4 was replaced by a holographic grating spectrograph, in which case the resolution was $\approx 2\ cm^{-1}$.

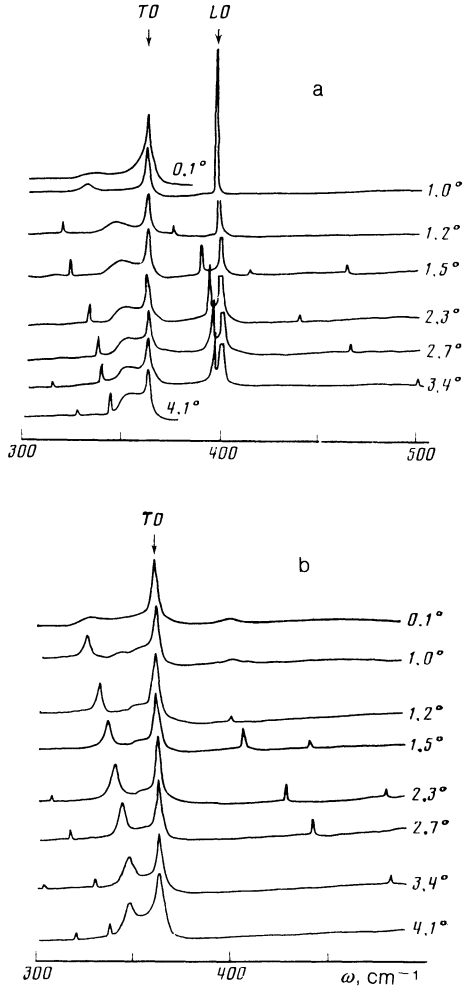


FIG. 2. Calculated spectra of RS by $p$ modes (a) and $s$ modes (b) of a GaP film at various scattering angles $\theta$.

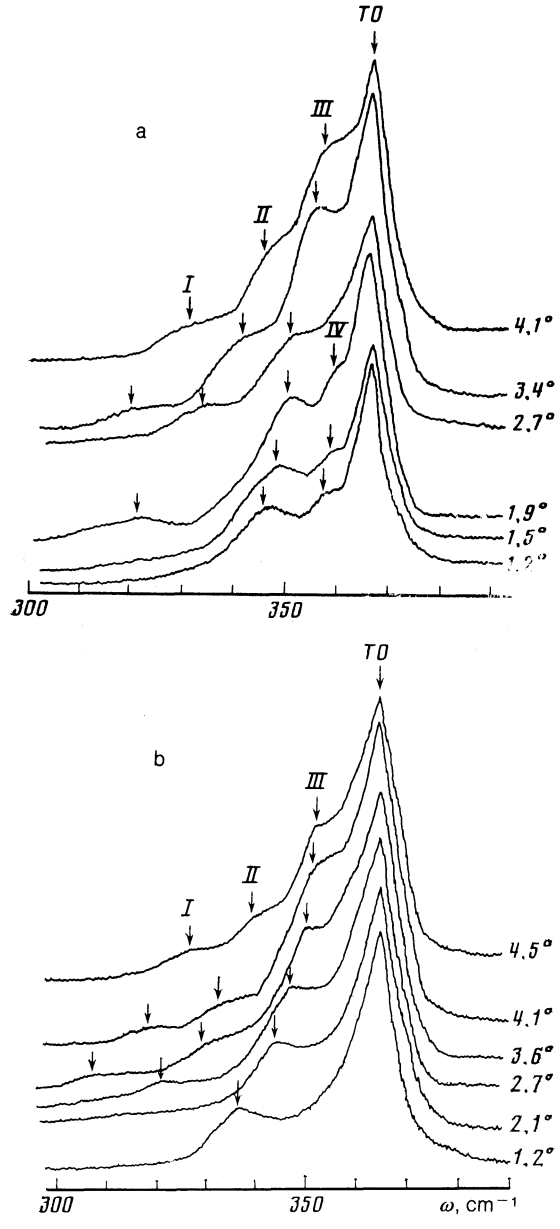


FIG. 3. Spectra of RS by $p$ modes (a) and $s$ modes (b) of the lower branches of the WM of a GaP film at various scattering angles: I–IV correspond to modes $m = 1$–4.

The RS by WM and IM was investigated by the forward-scattering procedure developed by us earlier for the observation of surface polaritons[5] using ring diaphragms.[7] The angular resolution of the diaphragms was 0.25°. A set of diaphragms covered the range of scattering angles $\theta$ outside the crystal from 0.5 to 4.5°.

The GaP-film surface, prepared by optically grinding a bulk crystal followed by polishing with diamond powder with grain size $\lesssim 0.5$ $\mu$m, was located in the (111) plane, while the directions [110], [112], and [111] served as the $x$, $y$, and $z$ axes. The film thickness was $6.8 \pm 0.5$ $\mu$m.

Since the RS-tensor form is known for this film geometry,[5] it is possible to determine analytically which of the modes ( $p$ or $s$) is observed in the particular scattering geometry. Type-$p$ modes are active in geometries in which the polarization $E^p$ of the excited vibration lies in the plane $\sigma$ which contains $\mathbf{k}_\parallel$ and the normal to the film surface. In the case of $s$-modes, $E^p \perp \sigma$. The experimental $p$ and $s$ modes are separable by the polarization measurements if $\mathbf{k}_\parallel$ is directed along the $x$ or $y$ axis (see Table I). To specify a definite direction of $\mathbf{k}_\parallel$ we used in the optical system, in addition to ring diaphragms, also a sector diaphragm, just as in the case of surface polaritons.[5]

## 4. EXPERIMENTAL RESULTS AND THEIR DISCUSSION

### 4.1. RS spectra and dispersion of waveguide modes

We investigated the WM dispersion separately for the $p$ and $s$ modes. To this end, the exiting radiation polarized along the $y$ axis was directed perpendicular to the plate (focused by an $F = 400$ mm lens) along the $z$ axis. The cutout of the sector diaphragm was chosen along the $y$ axis, so that the diaphragm passed light scattered by WM with wave vector $\mathbf{k}_\parallel \parallel y$. According to the table (geometries 7 and 8), it is possible to investigate in this case, by suitable choice of the polarization of the scattered light, either the $p$ mode ($\mathbf{E}_s \parallel \mathbf{y}$, $I_{yy}$) or $s$ modes ($\mathbf{E}_s \parallel \mathbf{x}$, $I_{yy}$).

The spectra of RS by WM of the lower branches at various scattering angles $\theta$ are shown in Fig. 3. The spectra show at frequencies $\omega < \omega_{TO}$, besides the $\omega_{TO}$ band, also maxima of WM bands, whose frequencies increase with increase of $\theta$. Raman scattering by WM of the upper bands was observed in experiment only at angles $\theta \gtrsim 1.4$, it was weaker than at the lower bands, and the maxima were shifted more

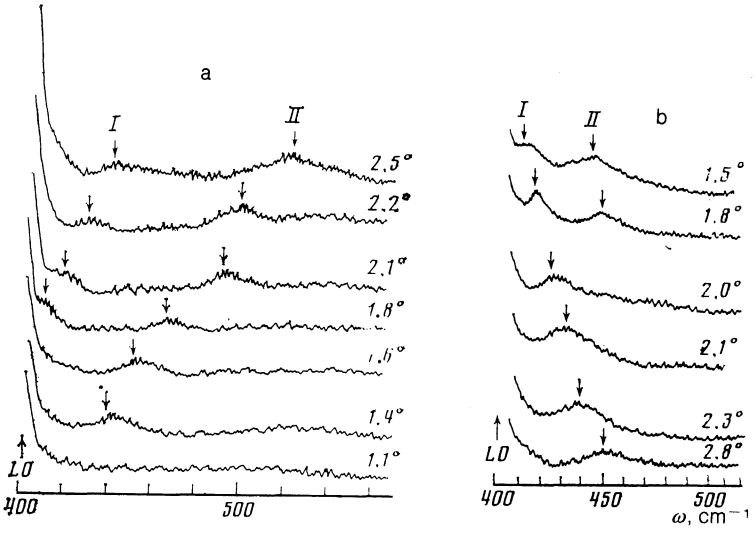


FIG. 4. Spectra of RS scattering by $p$ modes (a) and $s$ modes (b) of the upper WM branches of a GaP film at various scattering angles: I and II correspond to $m = 1$ and 2.

strongly with increase of $\theta$ (Fig. 4). In Fig. 5 are compared the experimental positions of the observed WM frequencies with the calculated dispersion [Eqs. (2) and (8)]. The calculated curves turn out to be sensitive to the choice of the dielectric function $\varepsilon(\omega)$.

The one-oscillator model $\varepsilon(\omega)$ with parameters $\varepsilon_\infty = 9.09, \omega_{TO} = 367\ \text{cm}^{-1}$ and $\omega_{LO} = 403\ \text{cm}^{-1}$ led to excessively large deviations. The many-oscillator dielectric function[12] gave better agreement with experiment, and the dispersion for the given $\varepsilon(\omega)$ is shown in Fig. 5 (solid lines). We have found the form of the function $\varepsilon(\omega)$ in the 300–380 $\text{cm}^{-1}$ region from the RS spectra of the GaP crystal used to produce the film. The vibrational Green's function obtained from real RS spectra[14] were used to determine the anharmonic parameters [the damping $\Gamma(\omega)$ and the anharmonic shift $\Delta^{(3)}(\omega)$], from which we were able to deduce the imaginary and real parts of $\varepsilon(\omega)$. This independent method of determining $\varepsilon(\omega)$ confirmed on the whole the validity of the many-oscillator model[12] for the GaP crystal in the 300–380 $\text{cm}^{-1}$ region. Let us point out the main features of the waveguide-mode dispersion.

1. In the region of the lower branches (Fig. 3), only several branches are observed (four for the $p$ modes and three for the $s$ modes) instead of an infinite number of WM.

2. There is no branch connected with $m = 0$ in the RS of either the lower or the upper branches.

3. Given $m$, the frequencies of the $s$ branches are systematically lower than those of the $p$ branches. Both branch types, however, approach the light line at almost the same point: the $p$ branches are tangent to the light line and the $s$ branches cross it (Fig. 5).

All these features correlate with the calculated dispersion and with the calculated RS spectra. Note that in the region of the upper branches we were able to observe only branches with $m = 1$ and 2. For the $p$ branch we observed at $m = 2$ a noticeable discrepancy between the experimental points and the calculated curve in the region $\omega > 480\ \text{cm}^{-1}$. It is possibly due to WM interaction with two-phonon states that fill the region from $\omega_{LO}$ to $\approx 800\ \text{cm}^{-1}$.

### 4.2 Intensity and damping of waveguide and interference modes

Whereas the $s$ modes are polarized parallel to the film surface, the $p$ modes can be polarized both perpendicular ($E_\perp^p$) and parallel ($E_\parallel^p$) to the film surface. The connection between $E_\perp^p$ and $E_\parallel^p$ is determined by the same relations as for surface polaritons,[3] viz., $E_\perp^p / E_\parallel^p = -k_\parallel / k_\perp$. Since $k_\parallel / k_\perp < 1$ (for GaP, e.g., $k_\parallel / k_\perp = 0.2$ at $\theta = 1.5$ and $\omega = 350\ \text{cm}^{-1}$), the intensities of the $p$ modes, determined by $E_\perp^p$ and $E_\parallel^p$, can be unequal. On this basis, quasi-selection rules were predicted,[3,6] according to which the $p$ modes determined by $E_\perp^p$ should have low intensity compared with the $p$ and $s$ modes determined by $E_\parallel^p$. To verify this assumption, we have investigated RS by WM at various scattering geometries.

Since the most intense mode in the WM spectra (Figs. 3 and 4) is that with $m = 3$, which determines in fact the form of the spectrum, we have investigated for simplicity integral spectra (without ring diaphragms), and recorded simultaneously light scattered from a set of angles 0.6–2.4°. In this case, however, the direction of $\mathbf{k}_\parallel$ was set with the aid of a sector diaphragm, and suitable polarizations $\mathbf{E}_L$ and $\mathbf{E}_s$ were chosen (Fig. 6). According to the table, different modes should appear in each of the spectra of Fig. 6, viz., a—$p(E_y^p) + p(E_z^p)$, b—$s(E_y^p + p(E_z^p)$, c—$s(E_x^p)$, d—$p(E_x^p)$. Actually, however, spectra of two types are observed. Spectra a and d are the same, since both contain only $p$ modes. Although the spectrum b is a sum of $s$ and $p$ modes, it is very close to the $s$-mode spectrum (spectrum c), indicating that $p(E_z^p)$ modes make a small contribution to spectrum b. The quasi-selection rules thus hold in first-order approximation. This conclusion is based on the change of the intensities of the bands near 345 $\text{cm}^{-1}$, which make up the spectra in Fig. 6. Analysis shows, however, that $k_\parallel \to k_\perp$ with decrease of frequency, and at $\omega < 300\ \text{cm}^{-1}$ we have $k_\parallel / k_\perp \sim 1$.

As seen from Figs. 2–4, the observed intensity distributions of the individual WM, as well as their positions, agree

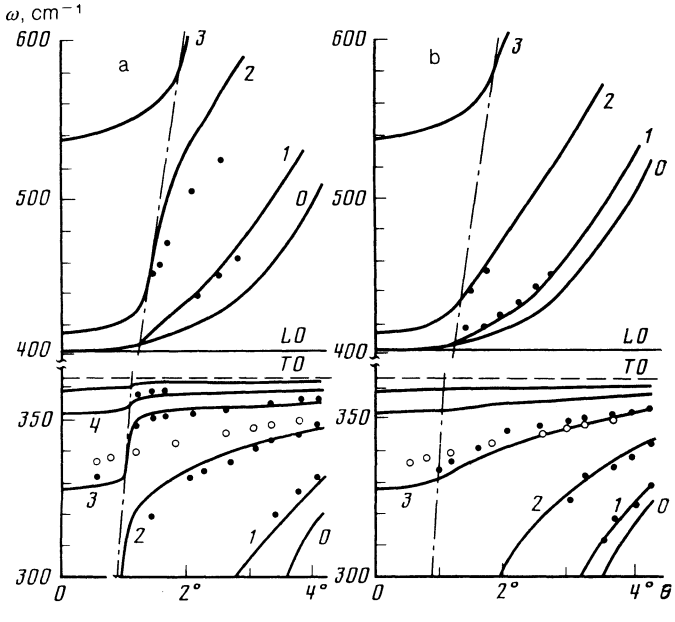


FIG. 5. Dispersion dependences of $p$ modes (a) and $s$ modes (b) of a GaP film: solid lines—calculated, ●—experimental points, dashed line—position of $TO$ phonon, dash-dot line—light line, $k = \omega/c$, ○—experimental points obtained for bulk polariton of GaP 350 $\mu$m thick.

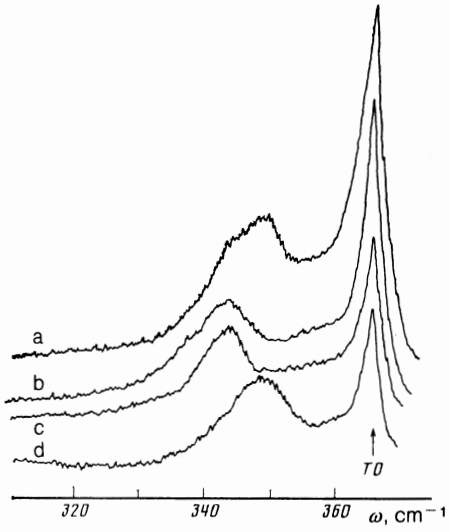


FIG. 6. Integral spectra of RS by WM of lower branches of a GaP film at various scattering geometries: a—$\mathbf{k}_{\parallel} \parallel \mathbf{y}$, $I_{xx}$; b—$\mathbf{k}_{\parallel} \parallel \mathbf{x}$, $I_{xx}$; c—$\mathbf{k}_{\parallel} \parallel \mathbf{y}$, $I_{xy}$; d—$\mathbf{k}_{\parallel} \parallel \mathbf{x}$, $I_{xy}$.

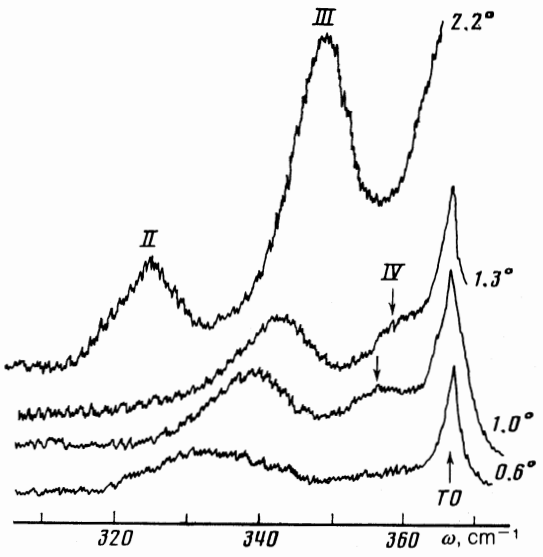


FIG. 8. Spectra of RS by WM and IM of $p$-type of lower branches of GaP film at various scattering angles.

with the calculation. In a comparison of the theoretical spectra with the experimental ones it must be recognized that the spectra observed are influenced not only by the instrumental function of the spectrometer but also by the finite gathering angle of the scattered light and by the deviation of the film surfaces from parallelism. For example, at the lower branches of the band the WM become rapidly narrower with decrease of $m$. Since the bands are broadened by instrumental distortions, the narrower WM bands in real spectra will have lower peak intensities than the calculated spectra. As follows from the calculations, the relative intensities are sensitive to $\varepsilon(\omega)$ and to the refractive indices $n_L$ and $n_s$, as well as to the film thickness. Figure 7 shows the spectra of RS by WM of a thick GaP film ($d = 10.5 \pm 0.5$ $\mu$m), where the two $p$ modes are of comparable intensity.

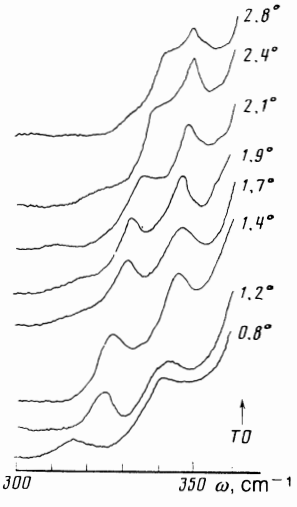


FIG. 7. Spectra of RS by WM of lower $p$-mode branches of a GaP film $10.5 \pm 0.5$ $\mu$m thick at various scattering angles.

To investigate the WM and IM damping, the RS spectra were obtained with $\approx 2$ cm$^{-1}$ resolution (Fig. 8). In this case the WM bands with $m = 2$ and $m = 3$ were well resolved on the lower branches and their widths could be estimated. At $\theta = 2.2°$ the observed width of the $p$ mode with $m = 3$ is $\approx 9$ cm$^{-1}$ (Fig. 8) and represents in fact the true width of the WM band, since both the spectrometer instrumental function and the angular instrumental function, the latter determined by the ingathering angle, are small. Recognizing that the damping of a phonon at the frequency of a WM with $m = 3$ ($\omega \approx 350$ cm$^{-1}$) is $\approx 8$ cm$^{-1}$, as found earlier from the polariton spectra,[15] it should be concluded that, if it is present at all, the WM-band broadening due to surface roughness and discussed in Ref. 9 is insignificant.

It follows from the calculated dispersion (Fig. 5) that at angles $\theta < 1°$ IM should be observed in the RS spectra. Actually at $\theta < 1°$ the quality of the spectra deteriorated noticeably, becoming blurred and less intense. At $\theta = 0.6°$ the width of the $p$ mode with $m = 3$ almost doubled (Fig. 8), a fact attributable to radiative damping of the IM. Since the IM frequency is practically independent of $\theta$ (Fig. 5), the instrumental distortions should be small and the broadening should correspond to an increased damping of the IM. Note that no spectra of RS by higher-branch IM could be obtained because of the exceedingly low intensity (calculation yields for $m > 1$ an intensity smaller by an order of magnitude than for lower branches).

## 5. CONCLUSIONS

The spectra of Raman scattering by waveguide and interference modes of a GaP film have been systematically investigated both theoretically and experimentally. General expressions that describe the spectrum of RS by natural vibrations of the film (by surface polariton, WM, IM, and *TO* and *LO* phonons) have been obtained, and the spectra at different scattering geometries for a GaP film calculated. Polarized RS spectra with good WM resolution, and also RS spectra with the $p$ and $s$ modes separated, were obtained for the first time, as was also RS by upper-branch WM and by

lower branch IM. The RS by upper-branch WM was observed in a region where GaP bulk polaritons are forbidden in RS. The features of the dispersion and of intensity of WM and IM have been analyzed. The validity of the quasi-selection rules of differently polarized modes in WM spectra is confirmed by experiment. Attention has been paid to the small influence of surface roughness on the WM line width. Comparison of the calculation with the experimental results has shown that the expressions describe satisfactorily the dispersion, intensity, damping and polarization of the WM and IM.

The authors thank V. M. Agranovich for a helpful discussion of the results.

[1]K. L. Kliewer and R. Fuchs, Phys. Rev. **144**, 495; 150, 573 (1966).
[2]V. V. Bryksin, D. N. Mirlin, and Yu. A. Firsov, Usp. Fiz. Nauk **113**, 29 (1974) [Sov. Phys. Usp. **17**, 205 (1974)].
[3]D. L. Mills and K. R. Subbaswamy, Progr. in Opt. **19**, 44 (1981).
[4]Surface Polaritons, V. M. Agranovich and D. L. Mills, eds., North-Holland, 1982.
[5]V. N. Denisov, B. N. Mavrin, and V. B. Podobedov, Zh. Eksp. Teor. Fiz. **92**, 1855 (1987) [Sov. Phys. JETP **65**, 1042 (1987).
[6]K. R. Subbaswamy and D. L. Mills, Sol. St. Comm. **27**, 1085 (1978).
[7]E. A. Vinogradov, G. N. Zhizhin, and V. A. Yakovlev, Zh. Eksp. Teor. Fiz. **77**, 968 (1979) [Sov. Phys. JETP **50**, 486 (1979)].
[8]D. L. Mills, Y. J. Chen, and E. Burstein, Phys. Rev. **B13**, 4419 (1976).
[9]J. B. Valdez, G. Mattei, and S. Ushioda, Sol. St. Comm. **27**, 1089 (1978).
[10]R. M. Pierce and S. Ushioda, J. de Phys. **45**, Coll. 5, 219 (1984).
[11]L. D. Landau and E. M. Lifshitz, *Electrodynamics of Continuous Media*, Pergamon, 1959.
[12]A. S. Barker, Phys. Rev. **165**, 917 (1968).
[13]W. L. Faust and H. Henry, Phys. Rev. Lett. **17**, 1265 (1966).
[14]V. N. Denisov, V. M. Mavrin, V. B. Podobedov, and J. F. Scott, Ram. Spectr. **14**, 276 (1983).
[15]T. A. Leskova, B. N. Mavrin, and Kh. E. Sterin, Fiz. Tverd. Tela (Leningrad) **18**, 3653 (1976) [Sov. Phys. Solid State **18**, 2127 (1976)].

Translated by J. G. Adashko